Journal of Solid and Fluid Mechanics (JSFM), 16(3): 1-5, 2026

Shahrood University of Technology

Journal of Solid and Fluid Mechanics (JSFM)

DOI: **10.22044/jsfm.2026.16536.3997**

Manufacturing Engineering of Iran

An Experimental Study on the Effect of Surface Roughness on the Impact of Newtonian Droplets on Spherical Surfaces

L. Razzaghi[1], M. Norouzi[2], M. H. Kayhani[3]

[1] MSc. Student, Mech. Eng., Shahrood Univ., Shahrood, Iran
[2] Prof., Mech. Eng. Dept., Shahrood Univ., Shahrood, Iran

*Corresponding author: L. Razzaghi: lale.razzaghi@shahroodut.ac.ir

Received: 07/21/2025 Revised: 11/20/2025 Accepted: 12/02/2025

Abstract

In this study, the dynamic behavior of Newtonian droplets composed of various glycerol–water mixtures impacting spherical surfaces with different roughness and diameters was experimentally investigated using high-speed imaging and image processing techniques. The effects of fluid viscosity, impact velocity, surface roughness, and diameter ratio (D^*) on droplet spreading, rebound, and splashing were evaluated. Results showed that lower viscosity led to increased maximum spreading ratio (β_{max}) and enhanced dynamic rebound, whereas higher viscosity caused greater energy dissipation, limited spreading, and weaker rebound. Increasing impact velocity resulted in higher β_{max} and delayed time to reach maximum spread. High surface roughness promoted splashing and instability during spreading, while greater surface curvature facilitated droplet expansion. The interaction between roughness and curvature revealed that curvature plays a more prominent role at low roughness, whereas roughness dominates at high levels. These findings highlight the combined importance of fluid rheology, surface geometry, and impact conditions in characterizing droplet dynamics on spherical surfaces.

Keywords: Droplet impact; Surface roughness; Spreading diameter; Newtonian fluid.

1. Introduction

The impact of liquid droplets on solid surfaces is a fundamental phenomenon in fluid dynamics with significant relevance to both natural processes and industrial applications. It plays a critical role in technologies such as inkjet printing, spray coating, aircraft icing, surface cooling, and fuel injection in internal combustion engines. Consequently, the detailed investigation of droplet dynamics upon impact has long been a subject of scientific interest. Early studies demonstrated that parameters such as impact velocity, surface tension, contact angle, and viscosity govern the extent of spreading, rebound, and splashing of droplets [1,2].

Classical models based on the Weber number describe the maximum spreading ratio primarily as a balance between inertial and capillary forces. These models perform well for low-viscosity liquids, where the empirical relation $D_{max} \approx D_0 We^{1/4}$ holds [3]. However, in viscous fluids, part of the kinetic energy is dissipated in overcoming viscous resistance, leading to reduced spreading and diminished accuracy of classical predictions. To address this limitation, modified models have been proposed that incorporate energy losses due to viscous and surface effects, thereby improving predictive capability [4,5]. Moreover, droplet impact has been shown to proceed through distinct stages—initial deformation, spreading, relaxation, and rebound—where wettability and surface roughness become increasingly influential in the later phases [6,7].

Surface roughness is another critical factor in droplet dynamics. On smooth surfaces, droplets spread more uniformly and exhibit stable rebound, whereas increased roughness enhances kinetic energy dissipation, induces instabilities in the lamella, and promotes crown-type splashing [8–11]. Experimental studies confirm that higher roughness reduces both the maximum spreading length and diameter [11]. To distinguish between prompt and crown splashing regimes, a modified Ohnesorge number has been introduced [12]. Beyond overall roughness, microstructural features such as grooves, pillars, and sharp edges significantly alter droplet behavior by modifying contact time, apparent contact angle, and splashing thresholds [13–21]. Dynamic parameters such as the maximum contact angle and spreading ratio (β) have also been identified as more reliable indicators for predicting splashing events [21].

Surface curvature exerts a similarly important influence. On convex surfaces, centrifugal forces enhance droplet expansion and increase the wetted area, while concave geometries accelerate retraction and limit axial spreading. Studies have shown that the diameter ratio between the target and the droplet (D*), impact velocity, and surface tension collectively determine the maximum spreading and rebound dynamics [22–28]. Compared to flat substrates, spherical surfaces promote larger contact areas and stronger outward spreading due to centrifugal effects [29,30]. Furthermore, wettability and environmental conditions such as temperature affect rebound and spreading behavior; for instance, higher wettability increases the spreading angle while reducing rebound probability [31,32].

Despite these advances, most previous investigations have assumed spherical surfaces to be smooth and homogeneous. In reality, spheres often exhibit varying degrees of roughness, which can fundamentally alter droplet dynamics by modifying flow pathways, film thickness, spreading rates, and rebound behavior. Addressing this gap, the present study aims to systematically examine the combined effects of surface roughness and curvature on the impact dynamics of Newtonian droplets, thereby providing deeper insight into droplet behavior on complex geometries.

2. Methodology

An experimental setup was developed to investigate the impact dynamics of single droplets on spherical surfaces with controlled roughness. Millimeter-sized droplets were generated using a syringe pump via the pendant drop method, providing high repeatability in the initial droplet diameter (D_0) and impact velocity (U) Spherical substrates with diameters (D_S) of 11, 18, and 25 mm were used to examine curvature effects, while surface roughness was systematically varied using sandblasting and chemical etching techniques.

Droplet impact events were recorded using a high-speed camera, and image sequences were processed with a custom-developed MATLAB code to extract droplet contours and spreading dynamics. The instantaneous spreading length ($l_{(t)}$) was measured from the processed images, and the spreading factor was defined as

$$\beta = \frac{l_{(t)}}{D_0} \quad (1)$$

where ($l_{(t)}$) denotes the time-dependent wetted length and (D_0) is the initial droplet diameter. Time was nondimensionalized using

$$t^* = \frac{t \cdot U}{D_0} \quad (2)$$

where (t) is time and (U) is the droplet impact velocity.

To characterize the impact regime, several dimensionless parameters were employed. The Weber number, defined as

$$We = \frac{\rho D_0 U^2}{\sigma} \quad (3)$$

represents the ratio of inertial forces to surface tension forces, where (ρ) is the liquid density and (σ) is the surface tension. The Reynolds number, given by

$$Re = \frac{\rho D_0 U}{\mu} \quad (4)$$

quantifies the relative importance of inertial and viscous effects, with (μ) denoting the dynamic viscosity of the liquid. The influence of viscosity relative to inertia and surface tension was further characterized by the Ohnesorge number

$$Oh = \frac{\mu}{\sqrt{\rho\sigma D_0}} \quad (5)$$

The effect of surface curvature was expressed using the dimensionless diameter ratio

$$D^* = \frac{D_S}{D_0} \quad (6)$$

where (D_S) is the diameter of the spherical substrate. Each experimental condition was repeated three times, and the reported results correspond to averaged values with relative uncertainties below 3%, ensuring the reliability and repeatability of the measurements.

3. Results and Discussion

The dynamic behavior of droplets during the spreading and receding phases was analyzed separately to investigate the effects of key parameters on the impact process. These parameters included Weber number, surface roughness, the ratio of target diameter to droplet diameter (using spherical targets of 11, 18, and 25 mm), and fluid viscosity. Experiments were conducted on spherical surfaces with varying roughnesses (Ra = 0.31, 0.77, 1.87, and 14.7 μm). Each test was repeated three times, with mean values reported; standard deviations were below 3%, confirming data reproducibility and experimental reliability. The spreading phase lasted only a few milliseconds, while the receding phase took significantly longer. Fluids used included water, glycerin, and their mixtures to cover a broad viscosity range.

3.1. Effect of Fluid Viscosity

Figure 3 shows the spreading dynamics of water–glycerin mixtures on an 18 mm diameter spherical surface with moderate roughness (Ra = 0.77 μm). Low-Oh fluids (G0, Oh = 0.002; G70, Oh = 0.052) experienced maximum radial spreading with $\beta_{max} \approx 3.2 \pm 0.05$ and exhibited oscillatory receding, indicating efficient kinetic-to-surface energy conversion. In contrast, high-Oh fluids (G90, Oh = 0.395; G100, Oh = 2.674) showed limited spreading and no oscillations due to viscous dissipation dominating the dynamics.

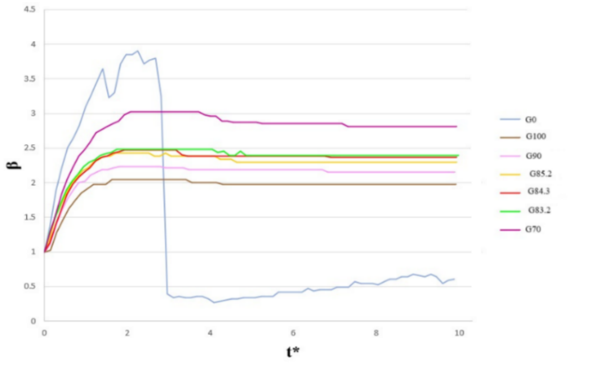

Figure 1- Effect of Fluid Viscosity on the Spreading Factor

3.2 Effect of Impact Velocity

Figure 4 depicts the effect of impact velocity on droplet G83.2 impacting a 25 mm diameter spherical metal target with Ra = 0.31 μm. Increasing velocity from 3.1 m/s (We = 711) to 4.1 m/s (We = 1244) enhanced β_{max} due to higher initial kinetic energy overcoming surface tension and viscous resistance. Figure 5 shows the combined effects of viscosity and velocity on β_{max} and spreading/receding times for G83.2, G84.3, and G85.2. Higher velocities resulted in thinner layers, faster radial spreading, and slightly higher β during receding, confirming that velocity strongly governs maximum spreading while viscosity modulates energy dissipation. Comparison with theoretical models (Clanet and Roisman) indicates that models considering both inertia and viscosity predict β_{max} more accurately.

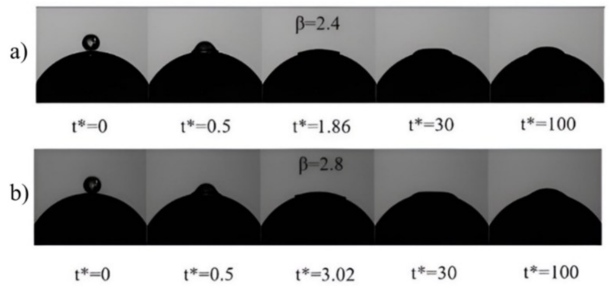

Figure 2- Impact of G83.2 droplets on a spherical target with diameter $D_S = 25$mm and surface roughness $Ra = 0.31\ \mu m$: (a) $We = 711(U = 3.1\ m/s)$, (b) $We = 1244(U = 4.1\ m/s)$.

3.3 Effect of Target-to-Droplet Diameter Ratio

Figure 6 shows G84.3 droplets impacting spheres of diameters 11, 18, and 25 mm (D* = 3.14, 5.14, 7.14) with constant droplet size and Ra = 0.31 μm. β_{max} increased with smaller D*, reflecting the enhanced tangential gravitational effect on surfaces with higher curvature.

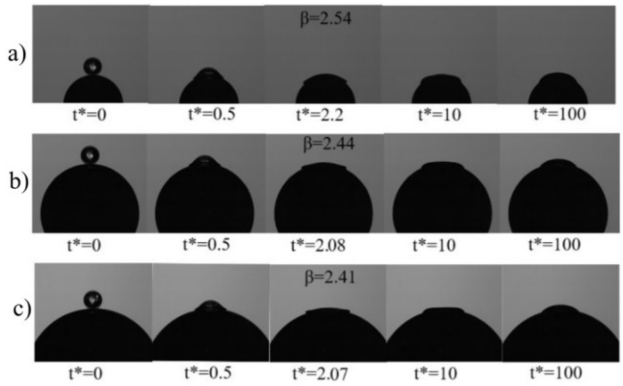

Figure 3- Impact of G84.3 droplets on a spherical target with surface roughness $Ra = 0.31\ \mu m$: (a) $D^* = 3.14$, (b) $D^* = 5.14$, (c) $D^* = 7.14$.

3.4 Effect of Surface Roughness

Figures 7 and 8 illustrate the role of surface roughness. On low-roughness surfaces (Ra = 0.31 μm), droplets spread uniformly to a stable $\beta_{max} \approx 4.8$ without splashing. On rougher surfaces (Ra = 1.87 μm), β_{max} slightly decreased to ≈ 4.5, and local instabilities induced early splashing. The interplay between roughness and D* was quantitatively described by the semi-empirical model:

$$\beta_{max} \approx 2.2 - 0.09(D^*) - 0.045\,\varepsilon \qquad (7)$$

where $\varepsilon = Ra/D_0$.

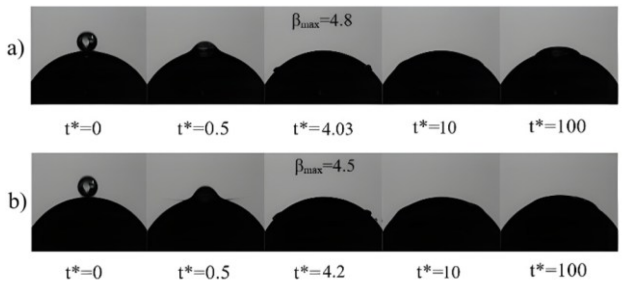

Figure 4- Impact of water droplet (G0) on a spherical target with $D_S = 25$ mmat $U = 3.1$ m/s: (a) $Ra = 0.31\ \mu m$, (b) $Ra = 1.87\ \mu m$.

3.4 Combined Effects of Velocity and Roughness

Figure 9 shows droplet G85.2 on 18 mm spheres at two roughness (Ra = 0.31 and 14.7 μm) and two impact velocities (3.1 and 4.1 m/s). Higher velocity consistently increased β_{max} for both roughness, whereas roughness mainly modulated the spreading uniformity and receding time. These results indicate that velocity dominates β_{max}, while surface roughness acts as a stabilizing factor controlling droplet shape and spreading dynamics.

Overall, maximum spreading increases with Weber number and decreases with viscosity and roughness, while the diameter ratio and surface roughness jointly determine spreading extent and dynamics.

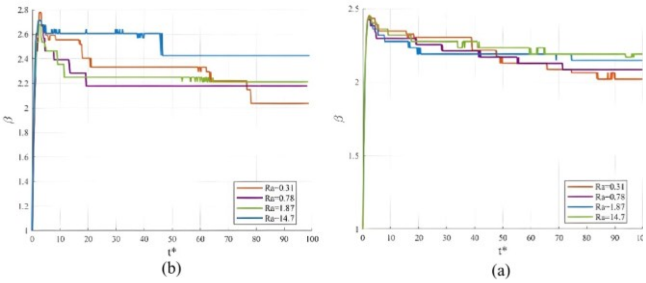

Figure 5- Impact of G85.2 droplets on a metallic sphere with diameter $D_S = 18$ mm at surface roughness values ranging from $Ra = 0.31$to 14.7 μm, under two impact velocities: (a) $U = 3.1$ m/s, (b) $U = 4.1$ m/s. Data are reported as mean values, with standard deviations below 0.08, confirming measurement reliability

4. Conclusions

The experimental investigation of droplet impact on spherical surfaces demonstrates that the spreading and receding dynamics are governed by the coupled effects of fluid properties, impact conditions, and surface characteristics. The results clearly indicate that increasing fluid viscosity, associated with higher Ohnesorge numbers, leads to a reduction in the maximum spreading factor (β_{max}) and suppresses oscillatory recoiling behavior. This trend reflects a transition from an inertia–capillary regime to a viscous–capillary regime, in which viscous dissipation dominates the energy balance and limits surface energy recovery.

Impact velocity was found to exert a strong influence on droplet dynamics. An increase in velocity, and consequently in the Weber number, enhanced β_{max} and delayed the time required to reach maximum spreading due to the higher initial kinetic energy of the droplet. Under high-Weber-number conditions, inertial forces overcome viscous and capillary resistance, reducing the relative damping effect of viscosity on droplet spreading.

Surface roughness significantly affected both the extent and stability of spreading. Smooth surfaces promoted more uniform spreading and higher β_{max} values, whereas increasing roughness introduced local disturbances at the lamella edge, triggering instabilities and secondary splashing. These findings highlight the dual role of surface roughness in both limiting the spreading width and promoting interfacial instabilities.

In addition, the ratio of target diameter to droplet diameter (D*) played a critical role in controlling the impact dynamics. A decrease in D* resulted in larger β_{max} values and shorter times to reach maximum spreading, attributed to the enhanced tangential flow component and more effective guidance of the liquid along highly curved surfaces. However, at higher surface roughness levels, the constraining effect of surface irregularities partially attenuated the influence of surface curvature.

Overall, the results demonstrate that the droplet impact behavior on spherical surfaces is controlled by the interplay between key dimensionless numbers (We and Oh) and geometric parameters (D* and surface roughness). By covering a wide range of experimental conditions, this study provides a comprehensive physical understanding of droplet dynamics on curved surfaces and offers a reliable basis for the development of improved numerical models and the optimization of industrial processes involving droplet impingement.

5. References

[1] Antonini, C., A. Amirfazli, and M. Marengo. Drop impact and wettability: From hydrophilic to superhydrophobic surfaces. *Physics of Fluids*, 2012. 24(10): p. 101301.

[2] Vadillo, D., et al. Dynamic contact angle effects onto the maximum drop impact spreading on solid surfaces. *Physics of Fluids*, 2009. 21(12): p. 122002.

[3] Clanet, C., et al. Maximal deformation of an impacting drop. *Journal of Fluid Mechanics*, 2004. 517: p. 199-208.

[4] Choudhury, R., et al. Maximum spreading of liquid drop on various substrates with different wettabilities. *Applied Surface Science*, 2017. 415: p. 149-154.

[5] Roisman, I.V., E. Berberović, and C. Tropea. Inertia dominated drop collisions. I. On the universal flow in the lamella. *Physics of Fluids*, 2009. 21(5): p. 052103.

[6] Rioboo, R., M. Marengo, and C. Tropea. Time evolution of liquid drop impact onto solid, dry surfaces. *Experiments in Fluids*, 2002. 33(1): p. 112-124.

[7] Pasandideh-Fard, M., et al. Capillary effects during droplet impact on a solid surface. *Physics of Fluids*, 1996. 8(3): p. 650-659.

[8] Tang, C., et al. Dynamics of droplet impact on solid surface with different roughness. *International Journal of Multiphase Flow*, 2017. 96: p. 56-69.

[9] Zhang, H., et al. How surface roughness promotes or suppresses drop splash. *Physics of Fluids*, 2022. 34(2): p. 022103.

[10] Liu, L., et al. Viscous droplet impact on rough surfaces. *International Journal of Multiphase Flow*, 2025: p. 105345.

[11] Chakaneh, J.Z., S. Javid, and M. Passandideh-Fard. Surface roughness effect on droplet impact characterization: Experimental and theoretical study. *Journal of Mechanical Engineering and Sciences*, 2019. 13(2): p. 5104-5125.

[12] de Goede, T., et al. Droplet splashing on rough surfaces. *Physical Review Fluids*, 2021. 6(4): p. 043604.

[13] Hao, J. Effect of surface roughness on droplet splashing. *Physics of Fluids*, 2017. 29(12): p. 122103.

[14] Xu, L. Liquid drop splashing on smooth, rough, and textured surfaces. *Physical Review E-Statistical, Nonlinear, and Soft Matter Physics*, 2007. 75(5): p. 056316.

[15] Range, K. and F. Feuillebois. Influence of surface roughness on liquid drop impact. *Journal of Colloid and Interface Science*, 1998. 203(1): p. 16-30.

[16] Wang, Z., K. Lin, and Y.-P. Zhao. The effect of sharp solid edges on the droplet wettability. *Journal of Colloid and Interface Science*, 2019. 552: p. 563-571.

[17] Abolghasemibizaki, M. and R. Mohammadi. Droplet impact on superhydrophobic surfaces fully decorated with cylindrical macrotextures. *Journal of Colloid and Interface Science*, 2018. 509: p. 422-431.

[18] Sapkal, N.P., et al. Experimental study of droplet splashing phenomena on hydrophobic micro-and micro/nano-textured surfaces. *Journal of Mechanical Science and Technology*, 2021. 35(11): p. 5061-5070.

[19] Yada, S., et al. Droplet impact on surfaces with asymmetric microscopic features. *Langmuir*, 2021. 37(36): p. 10849-10858.

[20] Jung, Y.C. and B. Bhushan. Dynamic effects of bouncing water droplets on superhydrophobic surfaces. *Langmuir*, 2008. 24(12): p. 6262-6269.

[21] Quetzeri-Santiago, M.A., A.A. Castrejón-Pita, and J.R. Castrejón-Pita. The effect of surface roughness on the contact line and splashing dynamics of impacting droplets. Scientific Reports, 2019. 9(1): p. 15030.

[22] Liu, Y., et al. Symmetry breaking in drop bouncing on curved surfaces. *Nature Communications*, 2015. 6(1): p. 10034.

[23] Deng, L., et al. Numerical study of water droplets impacting on cylindrical heat transfer pipes. *Engineering Applications of Computational Fluid Mechanics*, 2018. 12(1): p. 598-610.

[24] Sayyari, M.J., S.A. Naghedifar, and J.A. Esfahani. Pinch-off location and time during 2D droplet impact onto a wetted stationary cylinder using the lattice Boltzmann method. *Journal of the Brazilian Society of Mechanical Sciences and Engineering*, 2020. 42: p. 1-13.

[25] Wang, Y., Y. Wang, and S. Wang. Droplet impact on cylindrical surfaces: Effects of surface wettability, initial impact velocity, and cylinder size. *Journal of Colloid and Interface Science*, 2020. 578: p. 207-217.

[26] Arogeti, M., E. Sher, and T. Bar-Kohany. An experimental study of the events that follow a drop hitting a small surface. *Experimental Thermal and Fluid Science*, 2024. 150: p. 111067.

[27] Liu, X., et al. Study of the effect of surface wettability on droplet impact on spherical surfaces. *International Journal of Low-Carbon Technologies*, 2020. 15(3): p. 414-420.

[28] Bordbar, A., et al. Maximum spreading and rebound of a droplet impacting onto a spherical surface at low Weber numbers. *Langmuir*, 2018. 34(17): p. 5149-5158.

[29] Bakshi, S., I.V. Roisman, and C. Tropea. Investigations on the impact of a drop onto a small spherical target. *Physics of Fluids*, 2007. 19(3): p. 032102.

[30] Liu, X., X. Zhang, and J. Min. Maximum spreading of droplets impacting spherical surfaces. *Physics of Fluids*, 2019. 31(9): p. 092101.

[31] Khurana, G., N. Sahoo, and P. Dhar. Phenomenology of droplet collision hydrodynamics on wetting and non-wetting spheres. *Physics of Fluids*, 2019. 31(7): p. 072102.

[32] Banitabaei, S. and A. Amirfazli. Droplet impact onto a solid sphere: Effect of wettability and impact velocity. *Physics of Fluids*, 2017. 29(6): p. 062111.